

PAPER • OPEN ACCESS

Scheduling Scheme Optimization for Emergency Resources on a Deep-sea Considering Environmental Impacts

To cite this article: Ya-jie Wang *et al* 2022 *J. Phys.: Conf. Ser.* **2361** 012018

View the [article online](#) for updates and enhancements.

You may also like

- [Emergency Response Mechanism and Improvement of Hazardous Chemicals Accidents in Qing Yang City](#)
Ke Gai, Wanchun Chen and Shan Zhong
- [Planning and Implementation of Hazardous Waste Management Emergency Response Program – A Case Study of PT. X Medical Hazardous Waste Treatment](#)
M Candra Nugraha Deni and Aulia Shabirah
- [Study of flood mitigation system for improving the resilience of pluvial flood control of south Jakarta. \(Case study: Ciledug raya, Cipulir.\)](#)
Horas Yosua, Muhammad Syahril Badri Kusuma and Joko Nugroho



ECS
The
Electrochemical
Society
Advancing solid state &
electrochemical science & technology

DISCOVER
how sustainability
intersects with
electrochemistry & solid
state science research

Scheduling Scheme Optimization for Emergency Resources on a Deep-sea Considering Environmental Impacts

Ya-jie Wang, Jian-chun Fan*, Sheng-nan Wu

College of Safety and Ocean Engineering, China University of Petroleum-Beijing, Beijing, 102249, China

E-mail address: fjc6488@126.com (J.-c. Fan)

Abstract. An efficient and timely emergency response to a major accident is more challenging for the exploration and utilization of deep-sea oil and gas fields due to harsh external environment factors. An optimal solution is needed to tackle the external environment changes in the demand for emergency resources. To effectively balance emergency response time and the satisfaction of resource scheduling quantity, this paper proposes a multiple rescue points and multi-objective optimization model to address such challenges. Such model takes into account the environment factors involving wind speed and wave height caused by the variability of the deep-sea monsoon climate. Additionally, to handle the uncertainty of the resource demand at the accident sites, a linear programming and heuristic hybrid algorithm is proposed to help decision makers select the ideal routes and minimal scheduling time of deep-sea emergency resources, as well as the optimal operation season. A case study of a blowout accident is conducted to demonstrate the application of the proposed model and the real-world implications.

1. Introduction

As the demand for oil and gas grows continuously, the exploration and production of deep-sea oil and gas fields expand rapidly. Due to harsh external environments (including deep water, high waves, and strong winds) with complex processes and equipment, the development in deep-sea is far behind the inland counterparts. Meanwhile, sudden accidents on deep-sea oil and gas fields will bring geometrically larger damages than those on offshore fields. Once an accident occurs in the operation area, an efficient and timely supply of emergency resources is inevitably demanded. In this paper, resource storage terminal (RST) for deep-sea exploration are used to meet such demand. Specifically, the location of RSTs and the allocation of the required resources are two main challenges in this work.

Some complex mathematical models have been established to select the location to store resources. For example, [1] tried to maximize the efficiency of emergency resource distribution while minimizing the total construction cost of resource points and balancing the emergency demand of various demand points. With limited scheduling of static resources, they built an optimization model for resource locations under dynamic demands. [2] proposed a two-stage location-routing model with recourse for integrated preparedness and response planning under uncertainty. This model is used for risk management in disaster situations where there are uncertainties in demand and the state of the infrastructure. [3] proposed an index-based emergency response management system (IERMS) based on the Location Hazard Index (LHI) and the response time optimization model, which determines the locations of resource storage by solving the shortest response time and the optimal resource allocation in an emergency. [4] used a recent machine learning multiple layer perceptron (MLP) model and a Taguchi method to calibrate the MLP variables, combined an optimised pluvial flooding probability model with ideal location allocation methods on a geographic information system platform to construct the proposed



model for achieving accurate emergency response centres spatial planning. [5] took the maximum emergency efficiency as the objective function and constructed a location model of marine emergency material reserve based on timeliness, effectiveness, and differences in the demands for materials under accidents of various levels. [6] used a fully fuzzy-binary linear program to analyze the problem of maximum coverage locations. They proposed an augment-weighted Tchebycheff-based method to solve the problem. [7] proposed a Markov decision process (MDP) formulation for the stochastic road network recovery problem (SRNRP), and an approximate dynamic programming (ADP) approach to heuristically solve SRNRP. The authors considered a disaster scenario on a road infrastructure network that obstructs the flow of relief-aid commodities and search-and-rescue teams between critical service provided facilities and locations in need of these critical service.

Besides, demand-resource deployment has been comprehensively examined in the literature. For example, [8] discussed how the choice of different paths affects the efficiency and time uncertainty in scheduling. The problem of resource allocation and scheduling was solved using a decision support model and simulative analysis. [9] studied the Arctic region where there are few infrastructures with much difficulty in resource allocation. In their work, by allocating and scheduling public and private resources, a database and a dynamic network resource scheduling model were established to meet the needs for resources in the Arctic area. [10] used the spatial-temporal Poisson distribution to generate simulations of dynamic customers and analyzed their spatial and temporal characteristics in uncertain environments. In the end, the authors established a joint allocation model of multi-category resources that integrated the overall operation cost and vehicle fixed cost, which was proved to be better than the single category resource allocation model. [11] aimed at cutting down the response time toward events, as well as reduced the fleet operation costs and balanced the ship workload and emergency material dispatch. With the distribution plan of ships and materials under different target weights determined, an event type-based emergency model for material and ship distribution was established, and its effectiveness has been optimized. [12] judged the severity of oil spills by the established model of marine ships oil spill diffusion and created a resource scheduling model for different severity degrees of oil spills. The results revealed the earliest cleanse time for oil spill pollution and the optimal dispatch quantity of emergency materials. [13] reviewed the work done in D2D communication of resource allocation in the context of device to device communication, and the authors used the game theory to address the problem. Also provided the insight into the evolution that has been made in the area of resource allocation and highlight various open issues that needs to be addressed. [14] proposed a resource scheduling method for cooperative spatial target monitoring when detected spatial situations. Based on the task modes, objective functions, and the model and solution algorithms of the problem, the scheduling and target capacities, as well as the response time of the resource scheduling system were calculated. [15] considered a problem of supporting resource allocation decisions affecting multiple beneficiaries, and incorporated fairness in the form of welfare dominance, ensured that the resultant distribution of benefits. The authors introduced a new approach based on the paradigm of maximizing efficiency subject to constraints to ensure that the decision was acceptably fair. [16] used the single-type resources were to be assigned in the tree nodes such that the total weight in the rooted path from each leaf to the root equals its demand, and the authors set the aim was to minimize total costs of the allocated resources. [17] proposed a new differential evolution (DE) algorithm, called DEMIDRA, which each individual represented the resource allocation of a participating miner and the resources allocations of all participating miners constitute the whole population. The DE was adopted to optimize the resource allocation as for the optimization of the mining decision.

These efforts provide very important foundations for the research about RST locations and demand resource scheduling. However, as the drilling operations move to the deep-sea area, the risk of accidents in operations rises dramatically. In summary, special attention should be paid to how the external environmental factors interfere with the location selection and resource scheduling in emergency decision-making, and they are crucial to optimize decision-making and reduce risks. Therefore, in this paper, the main contributions are as follows:

1. A multi-objective optimization model for the deep-sea emergency resource scheduling is proposed to effectively balance emergency response time and the satisfaction of resource scheduling quantity.
2. The environment factors involving wind speed and wave height caused by the variability of the

deep-sea monsoon climate are taken into account.

3. A linear programming and heuristic hybrid algorithm is proposed to handle the uncertainty of the resource demand at the accident sites.

The remainder of this article is structured as follows. Section 2 a model to calculate the ship speed is introduced, and the multi-objective optimization model for RSTs location and scheduling in the deep-sea are established. This model can achieve the minimum emergency response time and satisfy the demand for emergency dispatching resources to the utmost extent. Then using a solution to the proposed model is given by LPHAL. Section 3 we are analyze the information about the wind field and wave heights in the deep-sea and using a case study of a blowout accident to demonstrate the application of the proposed model and the real-world implications. Section 4 the case study is discussed and some valuable features are summarized. Section 5 concludes the paper.

2. Methodology

2.1 Velocity formula

Deep-sea oil fields are especially susceptible to expansion and escalation. Besides, when an incident occurs, the meteorological, hydrographic, and sea conditions will interfere with the timeliness and reliability of emergency resource delivery by affecting the speed of rescue vehicles. When experiencing bad weather, the ship speed becomes subject to factors such as wind, windward angle, wave height, wavelength, wave-front angle, and the flow speed of wind-generated currents. Until now, the scientific field has offered a lot of findings of the speed of a ship sailing in wind and waves, such as the empirical ship stall equations proposed by James and the Central Institute of Shipping in the former Soviet Union. [18]

Specifically, the equation given by the Qingdao Meteorological Navigation Consortium was established based on that proposed by the former Soviet Maritime Research Institute in 1967, which includes the wave height quadratic coefficient k_2 and the wave direction coefficient k_3 . Besides, the Qingdao equation also refers to the B·C Clashock stall nomogram and an empirical coefficient G based on the actual ship measurements to calculate the stall amount [19]. Therefore, this paper applies the Qingdao equation to solve the actual speed of a ships in deep-sea, and Table 1 shows the description of each variable in the Eq. (1).

$$V_s = V - (k_1 h + k_2 h^2 - k_3 \alpha_1 h)(G - k_4 D_t V) \quad (1)$$

Table. 1 Scalar descriptions in the ship stall equation

Variable	Description	Variable	Description
V	speed of ships in still water	V_s	ship actual speed
h	wave height	G	empirical coefficient
D_t	actual displacement of the ship	k	each performance factor of the ship
α_1	the angle between the bow of the ship and the direction of the incoming waves		

2.2 Optimization model

When scheduling resources, a balanced resource distribution can prevent unnecessary losses to the emergency response. Therefore, the function of fuzzy affiliation in the triangular fuzzy \tilde{a}_{jk} is invoked in this paper, and the importance of different resources categories to the emergency point E_j , namely g_{jk} , was implemented to satisfy the demand for each type of resources to the utmost extent.

2.2.1 Model assumption. The contingency dispatch model for multiple resources and demand points in the deep-sea are set up with the following assumptions.

1) To find out the maximum emergency response time, each vessel will only distribute resources for one demand point in one voyage.

2) The carriers are all capable of meeting the voyage demand, and there are no halfway failures throughout any voyage.

3) RSTs have sufficient reserves of all types of resources to meet the demands at multiple

emergency points.

- 4) The ships travel safely during their voyages without ship accidents or piracy terrorism incidents.
- 5) All the ships share identical parameters.

2.2.2 Model. In this paper, the multistage decision-making model for the multi-objective optimization problem in the deep-sea is the primary concern. This model would seek solutions over a set of possible choices to optimize certain criteria. The minimum emergency response time $minT$ and the resource demand scheduling satisfaction $maxQ$ are expressed as follows.

Sets/indices

R	set of RSTs, $i \in R$
E	set of emergency points, $j \in E$
K	set of resource types, $k \in K$
R_{ik}	storage capacity of k resources in R_i
g_{jk}	importance of k resources to emergency point E_j
q_{ijk}	quantity of k resources distributed by R_i to emergency point E_j
c_{jk}	number of k resources received by emergency point E_j
\tilde{a}_{jk}	emergency point E_j triangular fuzzy number of resource requirement for category k
a_{jk}^l	emergency point E_j minimum value of demand for category k
a_{jk}^m	maximum demand of emergency point E_j for k resources
a_{jk}^r	emergency point E_j most likely value of demand for category k resources
$\mu(c_{jk})$	the demand satisfaction corresponding to c_{jk} is expressed by the fuzzy membership function of \tilde{a}_{jk}
S_{ij}	traveling distance between resource storage terminals R_i and emergency point E_j

Mathematical formulations Eq. (2) and (3) are the objective functions of T and Q , respectively. Objective function (2): Minimize the value emergency response time from R_i to E_j in case of an accident. Objective function (3): Maximize the demand satisfaction of the dispatched resource k when resource distribution is carried out.

$$minT = \sum_{j=1}^E (\max \sum_{i=1}^R \frac{S_{ij}}{V_s} X_{ij}) \tag{2}$$

$$maxQ = \sum_{j=1}^E \sum_{k=1}^K (\mu(c_{jk})g_{jk}) \tag{3}$$

$$s.t. X_{ij} = \begin{cases} 1, & \sum_{k=1}^K q_{ijk} > 0, R_i \text{ distribute } k \text{ resources to } E_j \\ 0, & \sum_{k=1}^K q_{ijk} = 0, R_i \text{ doesn't distribute } k \text{ resources to } E_j \end{cases} \tag{4}$$

$$\sum_{j=1}^E q_{ijk} \leq f_{ik} \tag{5}$$

$$c_{jk} = \sum_{i=1}^R q_{ijk} \geq a_{jk}^l \tag{6}$$

$$\tilde{a}_{jk} = (a_{jk}^l, a_{jk}^r, a_{jk}^m) \tag{7}$$

$$\mu(c_{jk}) = \begin{cases} \frac{c_{jk}-a_{jk}^l}{a_{jk}^r-a_{jk}^l}, & c_{jk} \in [a_{jk}^l, a_{jk}^r] \\ \frac{c_{jk}-a_{jk}^m}{a_{jk}^r-a_{jk}^m}, & c_{jk} \in [a_{jk}^r, a_{jk}^m] \\ 0, & else \end{cases} \tag{8}$$

$$g_{jk} \in (0,1) \tag{9}$$

Constraint (4) is used to control the resource transportation from R_i to E_j . When E_j is asking for resources from R_i , $X_{ij} = 1$; Otherwise, $X_{ij} = 0$.

Constraint (5) is used to constrain the number of resources dispatched by each RST. In other words, the actual supply of each type of material from any R_i cannot exceed the storage capacity of that material. Constraints (6) to (8) are the triangular fuzzy numbers of resources required by emergency point E_j .

When $c_{jk} < a_{jk}^l$, the number of class k resources from R_i to E_j cannot meet the emergency demands, making the whole schemes not feasible. However, if $c_{jk} > a_{jk}^m$, the amount of class k resources supplied by R_i to E_j will exceed the demand at E_j , resulting in a waste of resources and failure to obtain the

decision maker's utmost satisfaction. Therefore, constraint (8) is used to calculate the demand satisfaction of c_{jk} , and it is a constraint for the scheme feasibility.

Constraint (9) is a set of values to define the importance of category k resources to E_j .

This multi-objective optimization problem is an NP-Hard (Nondeterministic polynomial-Hard), namely, the solution will not be optimal for all objective functions at the same time. Therefore, the total objective function of the model is obtained by weighting each sub-objective linearly in this paper. However, since each sub-objective has a different magnitude, all of them must be dimensionless before subsequent operations. T_{max} and T_{min} are assumed the maximum and minimum values of objective function (2), while Q_{max} and Q_{min} are assumed the maximum and minimum values of objective function (3). After normalization, the two objective functions became:

$$f_T = (T_{max} - T) / (T_{max} - T_{min}) \quad (10)$$

$$f_Q = (Q_{max} - Q) / (Q_{max} - Q_{min}) \quad (11)$$

Where f_T and f_Q are the objective functions after the dimensionless processing of sub-objectives (2) and (3), respectively. Subsequently, assume the weight coefficients of emergency response time and resource dispatch satisfaction during deep-sea emergency rescue operations to be λ_T and λ_Q , respectively. These two coefficients must reside within (0,1), and $\lambda_T + \lambda_Q = 1$. With the two coefficients, the total objective function can be obtained.

$$\max F = \lambda_T f_T - \lambda_Q f_Q \quad (12)$$

2.3 Computational Procedure

Based on the features of deep-sea emergencies and the situation that the number of RST and emergency points remains low, the model is solved using a linear programming and heuristic algorithm language (LPHAL), and the specific steps are described below.

The shortest navigation range and route from R_i to E_j are found with the Dijkstra algorithm. Under constraints (4) to (9), a linear programming algorithm is used to find the extremums of emergency response time and resource dispatch satisfaction of Eq. (2) and Eq. (3), namely, T_{max} , T_{min} , Q_{max} , Q_{min} . These extremums are taken into Eq. (10) and (11) to obtain the values of f_T and f_Q . Subsequently, the expert evaluation method is used to find λ_T and λ_Q in the total objective function, which are then taken into Eq. (12).

3. Case study

The response time and the effectiveness of resource dispatch are two key indicators of emergency response at deep-sea. By analyzing the changes of wind speed and wave height caused by monsoon changed in the past 30 years as the interference factors of deep-sea emergency response, we can analyze the impact of different seasons on emergency response time and resource scheduling.

3.1 Hydrological information

Based on the WRF (weather research and forecasting) mesoscale climate model, Mike 21 software is used to simulate and analyze the wind field data of the deep-sea exploration area in the past 30 years. The simulation and analysis results are taken to calculate the wave field distribution in the area by the wave models of WAVEARCH III and Mike21 SW, and the workflow is shown in Fig.1.

3.1.1 Monsoon. The monsoon is a frequent condition in any deep-sea operation area, and the changes in wind speeds and directions affect the selection of RST locations. The wind field model is calculated within the region of 0.6°N , 103.2°E ~ 26.1°N , 126.2°E . Fig.2 shows the specific roadmap of RST candidate points (A ~ G) and emergency points (Accident Site1-3) during deep-sea oil and gas exploration. WRF simulation is used to get the changes of wind speed and direction at these points in different seasons, and the results are shown in Fig. 3.

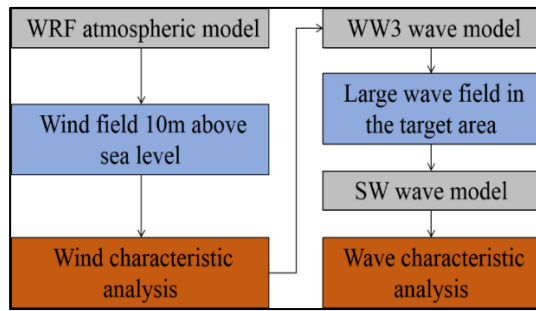


Fig.1 Flow chart of the calculation of wind and wave fields with the mathematical model



Fig.2 Regional road network of RST and emergency points

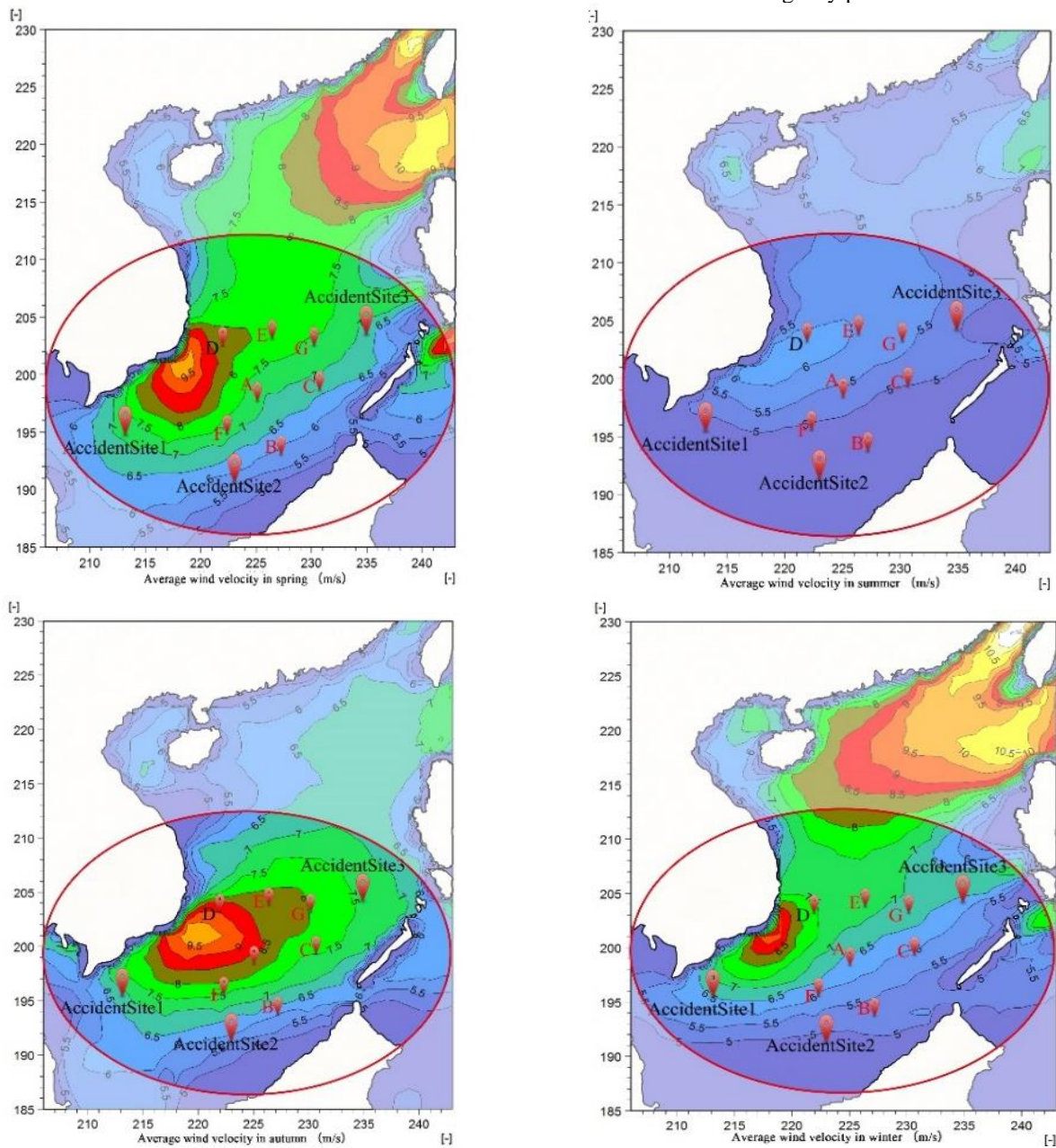


Fig.3 Wind speed and direction at the RST and emergency points in different seasons

From Fig. 3, it can be seen that the target exploration area is the least affected by the monsoon in summer, while in the other three seasons, the monsoon can bring significant impacts on the target area, especially

on the RST candidate points in the northwest of the region of interest. Moreover, in spring, autumn, and winter, the monsoon usually comes from the northeast, while the direction of monsoon origin shifts to the southwest in summer. Tables 2-5 show the information about the angles between the forward waves and bows at each node in different seasons.

Table.2 Angle between forward wave and bow in spring (α_1)

	A	B	C	D	E	F	G	Site1	Site2	Site3
A		165°	13°	63°	7°	170°	25°			
B	52°		35°			114°			150°	
C	135°	175°			65°		13°			
D	120°				79°	155°				
E	165°		115°	105°			45°			
F	23°	35°		5°				95°	145°	
G	150°		145°		125°					25°

Table.3 Angle between forward wave and bow in summer (α_1)

	A	B	C	D	E	F	G	Site1	Site2	Site3
A		25°	105°	105°	175°	15°	170°			
B	135°		170°			35°			5°	
C	55°	5°			95°		150°			
D	65°				105°	12°				
E	7°		45°	50°			120°			
F	170°	120°		175°				35°	30°	
G	3°		10°		40°					155°

Table.4 Angle between forward wave and bow in autumn (α_1)

	A	B	C	D	E	F	G	Site1	Site2	Site3
A		160°	12°	60°	10°	160°	20°			
B	47°		33°			105°			143°	
C	130°	170°			60°		10°			
D	123°				83°	160°				
E	150°		105°	100°			40°			
F	25°	35°		5°				90°	150°	
G	145°		145°		120°					30°

Table.5 Angle between forward wave and bow in winter (α_1)

	A	B	C	D	E	F	G	Site1	Site2	Site3
A		155°	10°	55°	5°	150°	20°			
B	45°		30°			100°			140°	
C	140°	170°			65°		15°			
D	125°				85°	140°				
E	160°		110°	95°			50°			
F	30°	40°		15°				90°	150°	
G	130°		125°		135°					20°

3.1.2 Wave. Monsoon is the main effective factor for RST and waves around the emergency points. When the northeast monsoon is prevailing, the NE (northeast) wave is dominant in October. From November to the next April, NE waves appeared at a percentage of more than 40%. Also, the wave heights showed a significant variation across months. Specifically, the maximum wave height was 1.8m in December, which dropped to 0.7m in April. When the southwest monsoon is on the way, S (south) and SW (southwest) waves prevail. In the data, S and SW waves appeared with a frequency of 40% - 50% in summer, and the monthly average wave height was 1.0-1.2m. During monsoon alternation, wave

directions fluctuate, and no obvious prevailing waves are observed. The minimum wave heights are found from April to May, and the wave direction varied.

The WAVEWATCH III model is applied to the region of 98.0~135.0°E, 8°S~27.0°N. Fig.4 shows the effective distribution of seasonal mean wave heights in that region after simulation, and Table 6 shows the wave height distribution of RST and emergency points in each season. The results suggest that wave height is obvious in spring, autumn, and winter (when NE monsoon is dominant) while being low in summer (when SW monsoon is dominant).

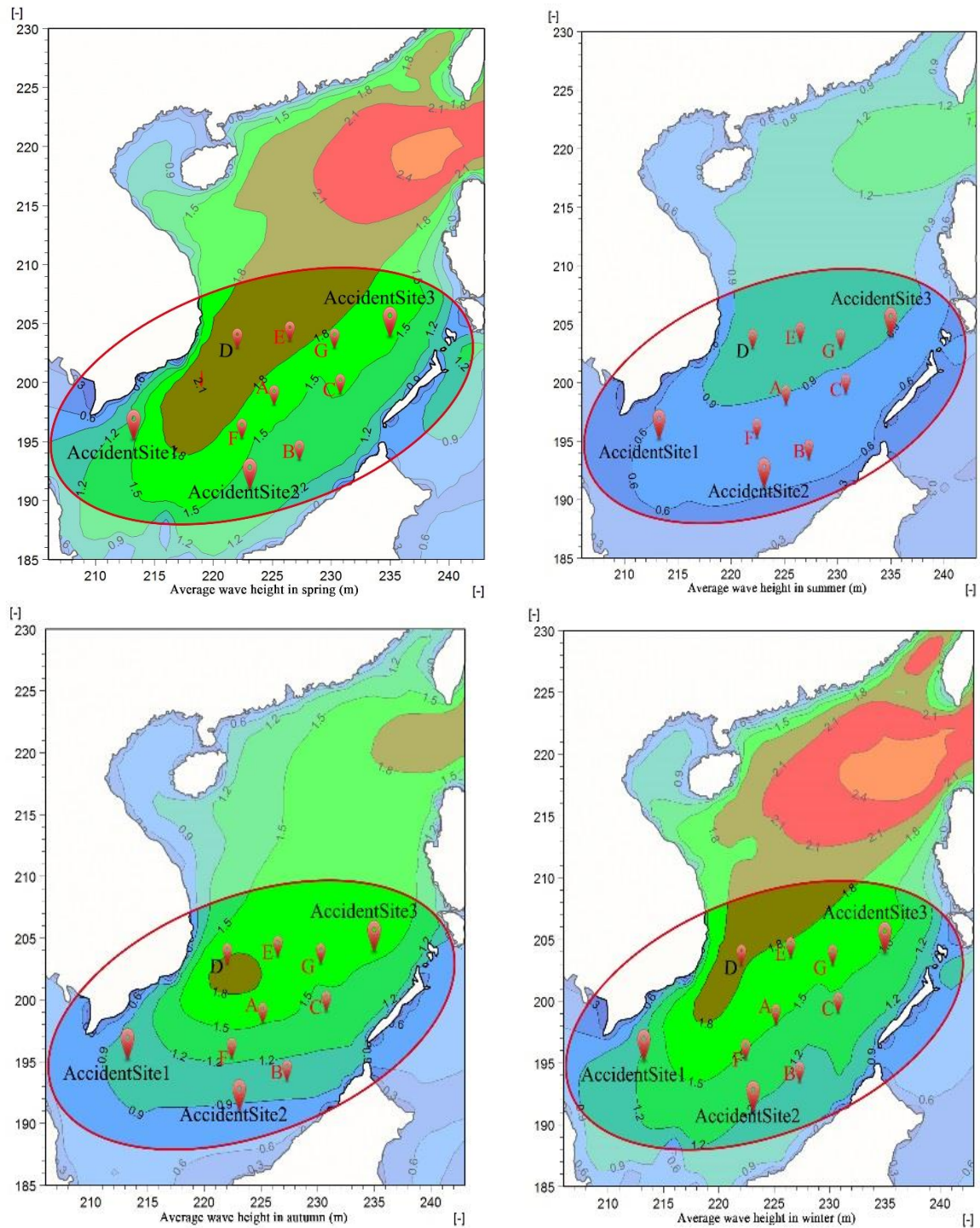


Fig.4 Effective distribution of mean wave heights by season

Table.6 Wave height distribution of RST and emergency points by season

h/m	A	B	C	D	E	F	G	Site1	Site2	Site3
-----	---	---	---	---	---	---	---	-------	-------	-------

Spring	1.6	1.3	1.5	2.4	2.2	1.6	1.7	1.5	1.4	1.6
Summer	0.85	0.65	0.8	1.1	1.2	0.7	1.0	0.65	0.6	0.9
Autumn	1.5	1.1	1.4	1.9	1.7	1.25	1.65	1.1	0.8	1.6
Winter	1.5	1.1	1.4	1.85	1.7	1.45	1.6	1.3	1.2	1.5

3.2 Example verification

This part aims to compare the changes in the sailing times and routes under different monsoons and wave conditions and analyze how these changes affect the distribution of RSTs for different materials. In this paper, a blowout accident is taken as an example, and the emergency relief materials belong to eight categories, namely, bop, barite, mud materials, cementing materials, crane, cutting machine, oil containment booms, and oil spill dispersants. Table 7 shows the importance of each emergency resource demonstrated by their expert scoring (g_{jk}). Table 8 shows the fuzzy number of resource demands at each emergency point based on the empirical knowledge (\tilde{a}_{jk}).

Table. 7 Importance of various types of emergency resources to the emergency points

Number	Name	Importance/ g_{jk}	Number	Name	Importance/ g_{jk}
1	bop	0.149	5	crane	0.114
2	barite	0.142	6	cutting machine	0.108
3	mud materials	0.129	7	oil containment boom	0.114
4	cementing material	0.136	8	oil spill dispersant	0.108

Table. 8 Fuzzy number of resource demands at the incident site (\tilde{a}_{jk})

	AccidentSite1	AccidentSite2	AccidentSite3
bop	(0,1,2)	(0,1,2)	(0,1,2)
barite	(70,100,120)	(60,85,100)	(50,95,120)
mud materials	(80,110,150)	(75,100,140)	(100,120,150)
cementing material	(95,120,145)	(80,100,130)	(90,120,150)
crane	(1,2,3)	(1,2,3)	(1,2,3)
cutting machine	(1,2,3)	(1,2,3)	(1,2,3)
oil containment boom	(800,1000,1500)	(700,900,1500)	(900,1200,1700)
oil spill dispersant	(5,10,15)	(6,10,13)	(7,12,16)

The ship speed is set to 14 knots and other parameters are $Dt=15197t, k_1 = 0.745, k_2 = 0.05015, k_3 = 4.5 \times 10^{-3}, k_4 = 1.35 \times 10^{-6}, G = 1.09, \lambda_T = 0.6, \lambda_Q = 0.4$. Both numbers are derived from expert evaluations. The verification is performed at Visual Studio 2012, Lingo 18.0, and MatlabR2016b under a Windows 7 computer with the host configuration of Intel corei5, CPU 2.5GHz, and a RAM of 12G. The actual ship speed in different seasons are solved based on Table 2 - 6 and Eq. (1). Fig.5 shows the sailing speed from RSTs to each node in different seasons. Among all four seasons, the ship speed in summer is the closest to that in still water, which is more conducive to emergency rescue.

With the LPHAL method described in Section 4.1, the minimum navigation time from RSTs to the emergency points, as well as the route variations are calculated for each season (as shown in Table 9). Besides, the extremums of T and Q are also calculated for each season under the constraints mentioned above being met (as shown in Table 10).

Based on these results, the number of resources of category k , namely, q_{ijk} , dispatched from R_i to E_j can be obtained, which is shown in Fig.6. The dispatch amounts of eight emergency resources in different seasons are reflected on the links between any two nodes, e.g. the amount of *barite* from point E to $Site3$ in *spring* is $40t$. A wireless segment link between two points means no resource transportation from R_i to E_j . Then the c_{jk} and X_{ij} can be found by q_{ijk} following a similar procedure, and the calculations are not repeated here.

Table. 9 Minimum sailing times and routes from R_i to E_j in different seasons

	Spring		Summer		Autumn		Winter		
	T_{min}/h	Route	T_{min}/h	Route	T_{min}/h	Route	T_{min}/h	Route	
Site1	A	4.53	A-F-Site1	3.54	A-F-Site1	3.24	A-F-Site1	4.63	A-F-Site1
	B	4.29	B-F-Site1	3.88	B-F-Site1	3.88	B-F-Site1	4.49	B-F-Site1
	C	6.52	C-B-F-Site1	5.83	C-B-F-Site1	5.80	C-B-F-Site1	6.61	C-B-F-Site1
	D	5.31	D-F-Site1	4.92	D-F-Site1	4.69	D-F-Site1	5.41	D-F-Site1
	E	7.40	E-D-F-Site1	6.10	E-D-F-Site1	6.38	E-D-F-Site1	7.29	E-D-F-Site1
	F	2.54	F-Site1	2.03	F-Site1	2.03	F-Site1	2.54	F-Site1
	G	8.12	G-A-F-Site1	7.76	G-A-F-Site1	7.51	G-A-F-Site1	8.13	G-A-F-Site1
Site2	A	4.26	A-B-Site2	3.28	A-B-Site2	3.25	A-B-Site2	4.46	A-B-Site2
	B	2.01	B-Site2	1.62	B-Site2	1.51	B-Site2	2.31	B-Site2
	C	4.14	C-B-Site2	3.27	C-B-Site2	3.53	C-B-Site2	4.14	C-B-Site2
	D	6.65	D-F-B-Site2	5.65	D-F-B-Site2	5.63	D-F-B-Site2	6.65	D-F-B-Site2
	E	6.79	E-C-B-Site2	5.81	E-C-B-Site2	5.78	E-C-B-Site2	6.59	E-C-B-Site2
	F	3.78	F-B-Site2	2.77	F-B-Site2	2.57	F-B-Site2	3.88	F-B-Site2
	G	6.35	G-C-B-Site2	5.40	G-C-B-Site2	5.34	G-C-B-Site2	6.65	G-C-B-Site2
Site3	A	5.38	A-G-Site3	4.25	A-G-Site3	4.38	A-G-Site3	5.63	A-G-Site3
	B	6.05	B-C-G-Site3	5.61	B-C-G-Site3	5.85	B-C-G-Site3	6.47	B-C-G-Site3
	C	3.88	C-G-Site3	2.79	C-G-Site3	2.88	C-G-Site3	4.08	C-G-Site3
	D	4.90	D-E-G-Site3	3.81	D-E-G-Site3	3.89	D-E-G-Site3	4.88	D-E-G-Site3
	E	3.20	E-G-Site3	2.74	E-G-Site3	2.90	E-G-Site3	3.19	E-G-Site3
	F	7.32	F-A-G-Site3	6.84	F-A-G-Site3	6.62	F-A-G-Site3	7.61	F-A-G-Site3
	G	1.62	G-Site3	1.09	G-Site3	1.32	G-Site3	1.72	G-Site3

Table. 10 Maximum and minimum values of each sub-objective function

	Target value	Response time /h	Demand satisfaction
Spring	Max.	38.31	1.848
	Min.	5.5	0
Summer	Max.	38.36	1.848
	Min.	5.38	0
Autumn	Max.	38.03	1.848
	Min.	5.5	0
Winter	Max.	38.3	1.848
	Min.	5.5	0

The deep-sea scheduling scheme of emergency resources obtained by this model can achieve the shortest emergency response time and the highest demand satisfaction. The target values of each seasonal sub-target and program running times are shown in Fig7, which could well meet the requirements of the emergency environment for rapid decision-making.

It should be noted that T_{obj} derived from this model is the sum of the time required to collect all supplies when incidents occur at all three incident points simultaneously. Table 11 gives the resource dispatch results when an incident happened at a single incident point. The dispatch of *cementing* materials for a sudden blowout at Site3 in autumn operations was used as an example to illustrate this model.

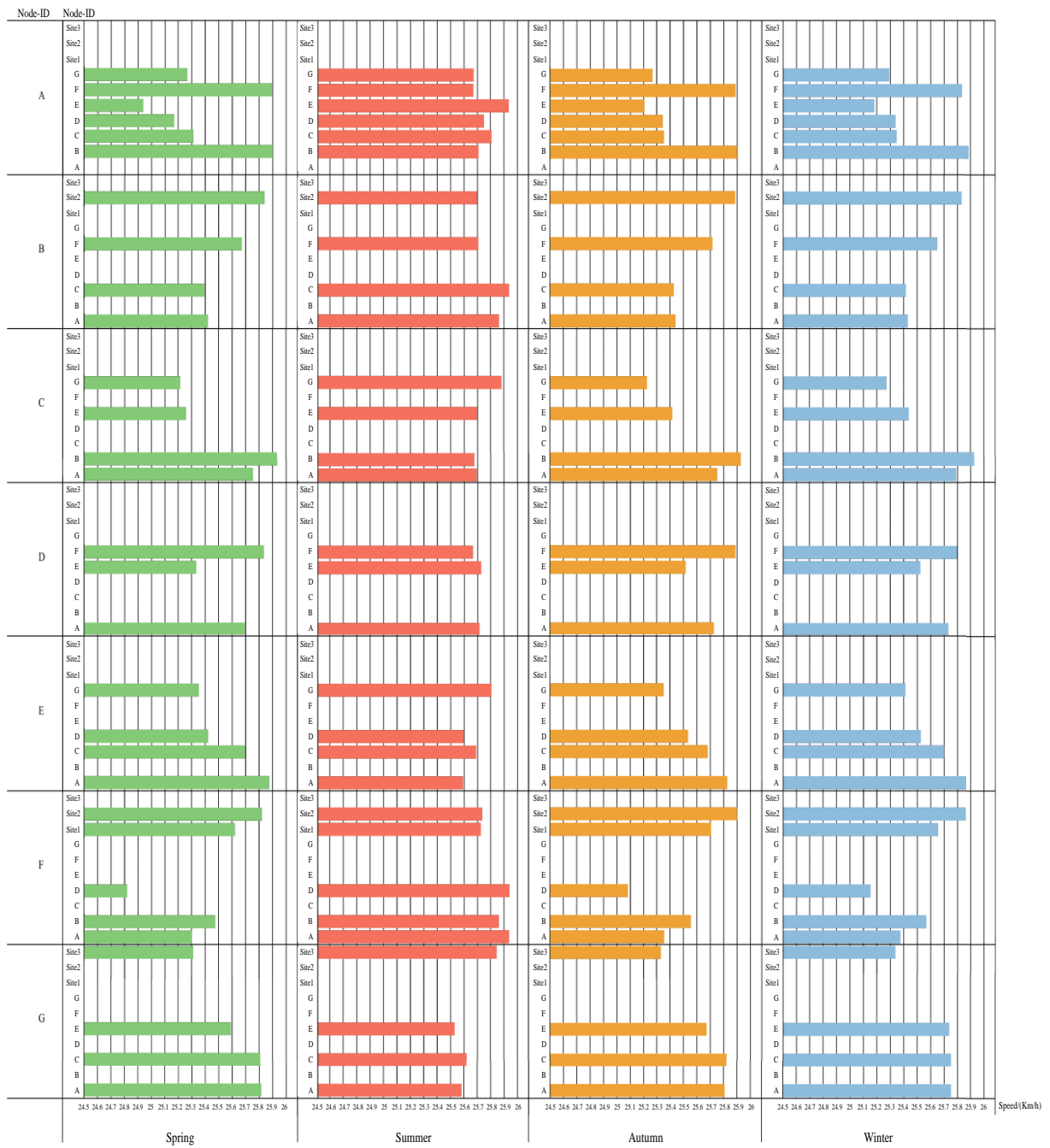
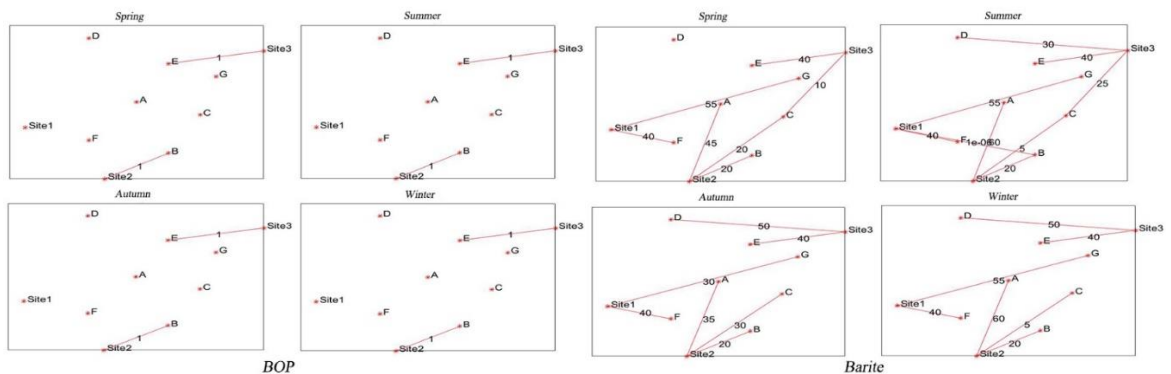


Fig.5 Variations in sailing speeds from RST to each node in different seasons



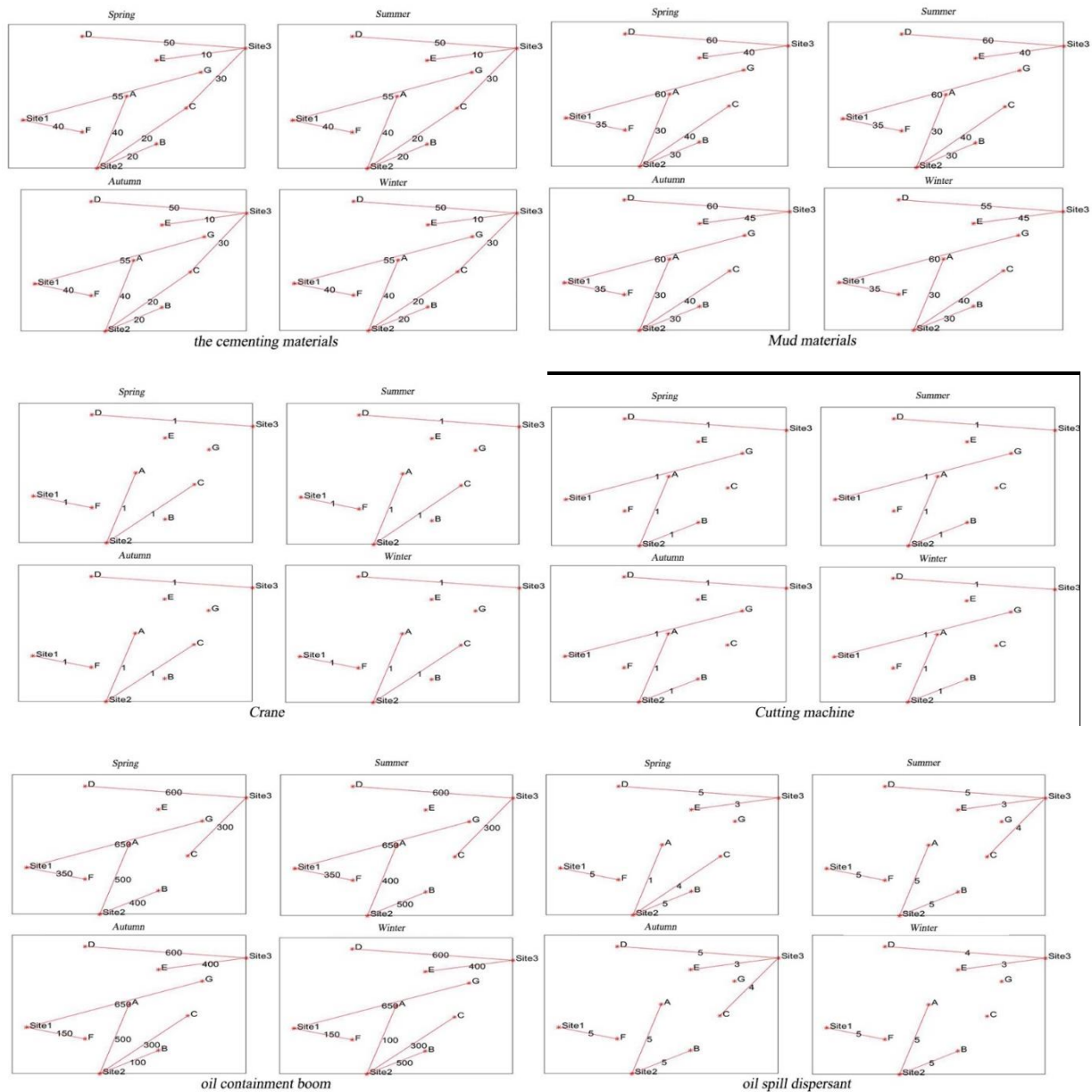


Fig.6 Comparison of resource scheduling options for blowout incidents by season in deep-sea

4. Discussion

According to the analysis in Section 4, the speed change from RSTs to each node in different seasons is shown in Fig. 4, which is determined by variables α_1 and h . The change of V_s can be used to determine the resource scheduling and the selection of RST in different seasons, as shown in Fig.5 and Table 10. In Table 10, the routes selection from RSTs to emergency points are not affected by seasonal factors, and the sailing time is shorter in summer and autumn. The resource allocation in Fig.5 shows that for the resource with small demands, the selection and scheduling quantity of RST are almost not affected by seasonal changes. For resources with large demands, the selection and scheduling quantity of RSTs are greatly affected by seasonal changes, and the scheduling results in autumn and winter are almost the same. To sum up, the operation time window from April to September every year are more suitable for deep-sea oil and gas field exploration and development.

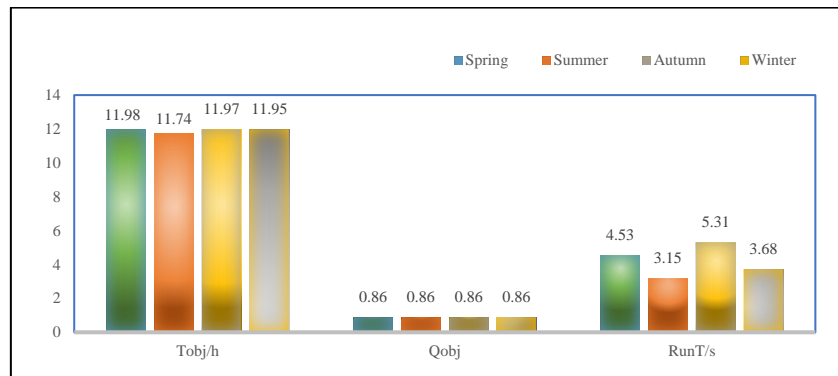


Fig.7 Comparison of sub-target values and running times by season

Table.11 an example of the resource dispatch

RST	Route	Time/h	Dispatch quantity/t
R_C	C-G-Site3	2.88	30
R_D	D-E-G-Site3	3.89	50
R_E	E-G-Site3	2.90	10

5. Conclusions

In this research, the selection of emergency routes and the dispatch of emergency resources in the deep-sea are studied based on the variations of wind speed and wave height in different seasons. Considering the changes of monsoon, the ship stall equation proposed by the Qingdao Meteorological Navigation Consortium of China is cited here. Based on the triangular fuzzy function, a deep-sea emergency resource dispatch model is proposed for a small number of RSTs to achieve minimum emergency response time and maximum resource dispatch satisfaction. The proposed model is validated with the LPHAL algorithm in an assumed blowout incident. Our model accomplished three objective: (1) Addressing the fuzzy uncertainty of the resource demands at the accident points, and the supply of each point are different due to the change of season. (2) The time and routes to dispatch resources in deep-sea emergencies at multiple rescue and accident points are determined. (3) According to the case study, the response time of summer is the shortest among the four seasons, and the resource dispatch satisfaction is the highest. Therefore, summer is the most preferred season for drilling operations.

The study provides a tool for analyzing and refining the siting and configuration of deep-sea emergency RSTs, making it important for marine systems in exploration areas that are vulnerable to natural factors, such as the South China Sea and North Atlantic Ocean.

Three directions are recommended for future work: (1) Based on the response time models, the effects of monsoons will be replaced by those of typhoons. Typhoons of different levels should be analyzed to better describe the impact of weather factors on the dispatch of deep-sea emergency resources. (2) Change the transport means, such as helicopters. We will collected more field data to diversify the choice of transportation means and make the model produce more practical results. (3) Improvements to the model are still to be made. In the future, data about the world's oceans should be included, and the user only needs to ensure the accuracy and reliability of the input parameters to start intelligent analysis and calculation, which is more conducive to the application of the model in the field.

Acknowledgements

Funding: The authors are grateful to China National Deep-sea Oil Corporation (CNOOC) for financial support to this work.

Reference

- [1] Gao, X, 2012. Research on the optimization methods of large-scale emergency rescue resources layout and scheduling. Jilin Univ. (in Chinese).
- [2] Akil M. Caunhye, Zhang, Y., Li, M., Nie, X.,2016. A location-routing model for prepositioning and distributing emergency supplies. Transp. Res. Part E. 90,161-176.

- [3] Yousuf Rebeeh, Shaligram Pokharel, Galal M. Abdella, Abdelmagid Hammuda, 2019. A framework based on location hazard index for optimizing operational performance of emergency response strategies: The case of petrochemical industrial cities. *Saf. Sci.* 117, 33-42.
- [4] Hossein Mojaddadi Rizeei, Biswajeet Pradhan, Maryam Adel Saharkhiz, 2019. Allocation of emergency response centres in response to pluvial flooding-prone demand points using integrated multiple layer perceptron and maximum coverage location problem models. *Int. J. Disaster Risk Reduct.* 38, 101205.
- [5] Zhang, L., Lu, J., 2019. Location of maritime emergency supplies repertoires considering risk uncertainty. *Chin. Saf. Sci. J.* 9, 173-180.
- [6] Manuel Arana-Jiménez, Víctor Blanco, Elena Fernández, 2020. On the fuzzy maximal covering location problem. *Eur. J. Oper. Res.* 283, 692-705.
- [7] Aybike Ulasan, Özlem Ergun, 2021. Approximate dynamic programming for network recovery problems with stochastic demand. *Transp. Res. Part E.* 151, 102358.
- [8] Duncan T. Wilson, Glenn I. Hawe, Graham Coates, Roger S. Crouch, 2014. Evaluation of centralized and autonomous routing strategies in major incident response. *Saf. Sci.* 79, 80-88.
- [9] Martha Grabowski, Christopher Rizzo, Travis Graig, 2016. Data challenges in dynamic, large-scale resource allocation in remote regions. *Saf. Sci.* 87, 76-86.
- [10] Ge, X., Xue, G., 2019. Multi-products joint distribution vehicle routing optimization with uncertain circumstance. *Comput. Eng. Appl.* 55, 264-270.
- [11] Zhu, X., Chen, C., 2019. Multi-objective optimization of marine emergency resource dispatching. *Navig. Chin.* 8, 46-51.
- [12] Chen, Z., 2020. Research on the optimization of emergency materials scheduling in maritime oil spill accident. *Dalian Marit. Univ.* (in Chinese).
- [13] Roopsi Rathi, Neeraj Gupta, 2020. Game theoretic and non-game theoretic resource allocation approaches for D2D communication. *Ain Shams Eng. J.*
- [14] Zhuang, H., Pan, T., He, Z., 2020. Method of resource scheduling for space object cooperative surveillance using Tabu Genetic Algorithm. *Spacecr. Eng.* 8, 46-51
- [15] Nikos Argyris, Özlem Karsu, Mirel Yavuz, 2021. Fair Resource Allocation: using Welfare-based dominance constraints. *Eur. J. Oper. Res. EOR*, 17212.
- [16] Nir Halman, Shmuel Wimer, 2021. Resource allocation in rooted trees subject to sum constraints and nonlinear cost functions. *Inf. Process. Lett.* 170, 106114.
- [17] Yong Wang, Chun-Rong Chen, Pei-Qiu Huang, Kezhi Wang, 2021. A new differential evolution algorithm for joint mining decision and resource allocation in a MEC-enabled wireless blockchain network. *Comput. Ind. Eng.* 155, 107186.
- [18] Zhang, Y.S., Lu, Y.Q., Cai, F., Shi, A.G., 2005. The comparison of several computing methods of ship's loss. *Mar. Technol.* 1, 7-9.
- [19] Wang, M.R., 2010. The study on the scheduling of rescuing resources for marine perils. *Dalian Marit. Univ.* (in Chinese).